

Article

Reactive Sputter Deposition of Ga₂O₃ Thin Films Using Liquid Ga Target

Marcell Gajdics *, Miklós Serényi, Tamás Kolonits , Attila Sulyok, Zsolt Endre Horváth and Béla Pécz 

Institute for Technical Physics and Materials Science, Centre for Energy Research, H-1121 Budapest, Hungary; sulyok.attila@ek-cer.hu (A.S.); horvath.zsolt.endre@ek-cer.hu (Z.E.H.)

* Correspondence: gajdics.marcell@ek-cer.hu

Abstract: Ga₂O₃ is a promising material in the optoelectronics and semiconductor industry. In this work, gallium oxide thin films were deposited via radio frequency (RF) sputtering, using a liquid Ga target. The reactive sputtering was carried out using different oxygen flow rates and DC target potentials induced via the RF power. The thickness of the samples varied between 160 nm and 460 nm, depending on the preparation conditions. The composition and the refractive index of the layers were investigated via energy-dispersive spectroscopy, X-ray photoelectron spectroscopy, and spectroscopic ellipsometry, respectively. It was found that, through the use of a lower DC target potential, a better film quality and higher oxygen content can be achieved. The reactive sputtering was modeled based on the Berg model, with the aim of determining the sputtering yields and the sticking coefficient. It was shown that an increase in DC target potential leads to the preferential sputtering of gallium.

Keywords: reactive sputtering; gallium oxide; thin film; liquid gallium



Citation: Gajdics, M.; Serényi, M.; Kolonits, T.; Sulyok, A.; Horváth, Z.E.; Pécz, B. Reactive Sputter Deposition of Ga₂O₃ Thin Films Using Liquid Ga Target. *Coatings* **2023**, *13*, 1550. <https://doi.org/10.3390/coatings13091550>

Academic Editor: Alexandru Enesca

Received: 24 July 2023

Revised: 26 August 2023

Accepted: 1 September 2023

Published: 5 September 2023



Copyright: © 2023 by the authors. Licensee MDPI, Basel, Switzerland. This article is an open access article distributed under the terms and conditions of the Creative Commons Attribution (CC BY) license (<https://creativecommons.org/licenses/by/4.0/>).

1. Introduction

Gallium oxide (Ga₂O₃), as an ultrawide bandgap semiconductor, has numerous potential applications in the fields of electronics and optoelectronics. It is a promising material for transistors and rectifiers in high-power electronics [1,2], as well as for solar-blind UV photodetectors and photodiodes [1–3]. In addition, as was recently demonstrated, it can also be utilized in gas-sensing applications [4].

Several processing techniques, from bulk growth methods to thin-film formation procedures, have been developed to synthesize Ga₂O₃ [1,2,5]. Among the film formation techniques, molecular beam epitaxy [6], metal–organic chemical vapor deposition [7], halide vapor phase epitaxy [8], pulsed laser deposition [9], mist-chemical vapor deposition [9], and sputtering [5] are the most commonly used methods. Sputtering is a frequently used technique, mainly because it offers the possibility of depositing highly uniform layers at low temperatures [10–12]. Ga₂O₃ films prepared in this way have demonstrated the potential to be used as a material in solar-blind UV photodetectors [3,13,14]. Sputtering can be carried out under different deposition conditions/parameters. These have a significant influence on the properties of the films [5,15], and also enable the control of these properties. For the deposition of gallium oxide, most often, a ceramic Ga₂O₃ target is used. As it is non-conductive, a radio frequency power source should be utilized. Sputtering such a Ga₂O₃ target in an Ar atmosphere usually leads to oxygen-deficient films [16,17]. Hence, in many cases, an Ar + O₂ atmosphere is used during deposition [14,15,18–20]. The investigations on the reactive sputtering of Ga targets are scarce, mainly due to the low melting point (T_m = 30 °C) of gallium. Only one recent study could be found on the preparation of Ga₂O₃ films using the reactive sputtering of liquid Ga [21].

The aim of this work was to study the sputtering process of a liquid Ga target during the deposition of gallium oxide films. The modeling of the reactive sputtering process was

carried out based on the Berg model [22,23]. The sputtering parameters, such as the partial sputtering yields and the sticking coefficient, were determined. The dependence of the composition and the refractive index of the deposited films on the sputtering conditions was also investigated. Finally, a comparison between the deposition of gallium oxide from a liquid Ga target and ceramic Ga_2O_3 targets was performed.

2. Materials and Methods

2.1. Sample Preparation

The high-purity gallium (Alusuisse, purity 99.9999%) was placed on the lower target area of a Leybold Z400 RF sputtering device, in a circular crucible fabricated from a 0.2 mm Ni plate (see Figure 1). The diameter of the container was 75 mm, and the height of its side wall was about 3 mm. This shape fitted well on the copper target holder of the sputtering device, which was water-cooled, and ensured the coupling of the RF power.

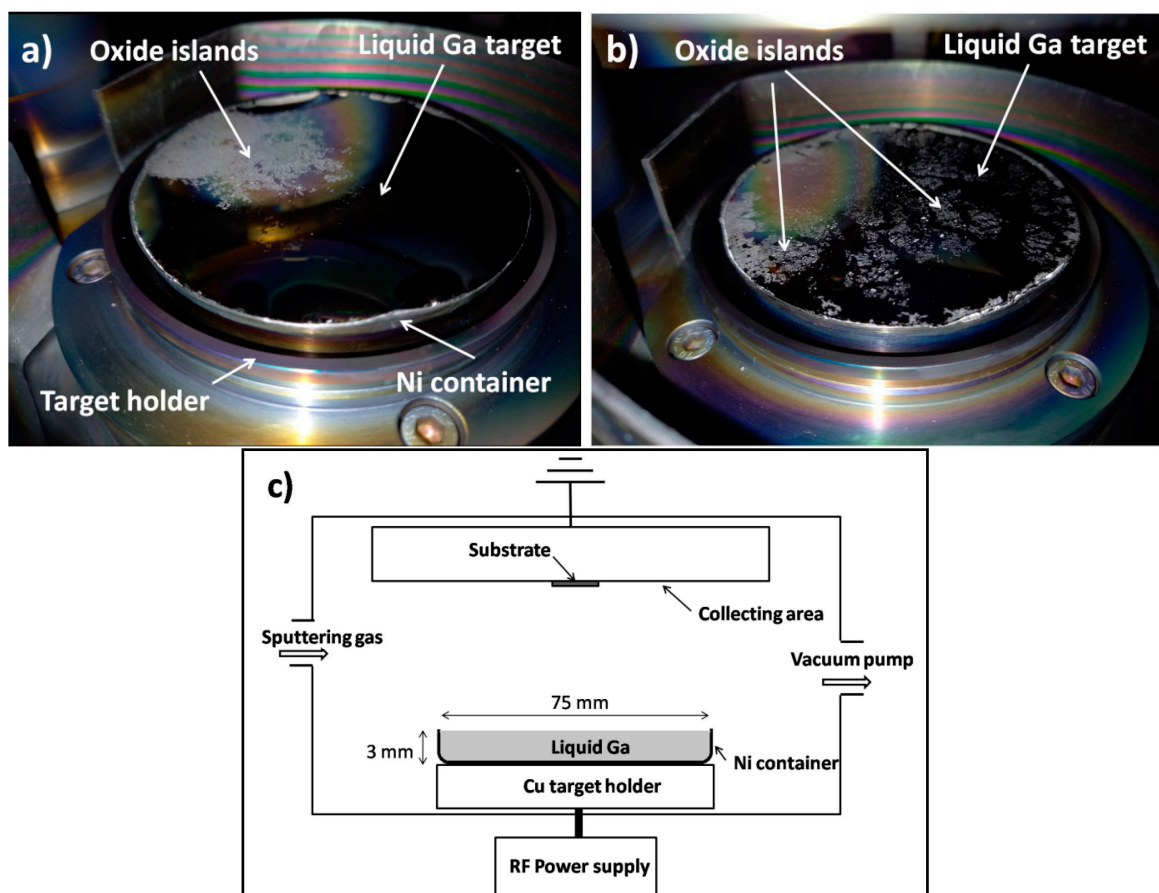


Figure 1. Photographs of the liquid Ga target in a Ni container inside the sputtering chamber, after sputtering at an oxygen flow rate of 12 sccm (a), and 32 sccm (b), and a schematic representation of the experimental setup (c).

The 3 mm wall height ensured that the relatively small amount of Ga, which is liquid at 30 °C, but was mostly supercooled during the manipulations, completely covered the diameter of the 75 mm target. The target was in a liquid state during sputtering, as verified through visual inspection. Due to the high surface tension of Ga in the Ni container, and the moderate wettability of the Ni interface, it easily breaks up into islands. To avoid this, we used a technique (the so-called fluxless oxide remover) similar to active soldering. The mechanical activation required to remove the oxide layer from the Ni surface can be performed with a brush (e.g., a stainless wire brush or steel spatula) or via ultrasonic vibration. In our case, the wall of the container was heated from the outside with an electric heater to 350 °C under ambient conditions, while the Ni surface in contact with the Ga

melt was scraped with a steel spatula, until a continuous surface covered with the melt was obtained (at least 15 min of mechanical activation).

The liquid Ga target was reactively sputtered using the above-mentioned Leybold Z400 RF sputtering device, operated at a frequency of 13.56 MHz. The reason for our choosing this device was that it has a bottom target holder, which is necessary for the liquid target. However, this experiment can also be performed using pulsed DC sputtering or HiPIMS devices equipped with a bottom target placement option, as well. For all deposition experiments, the sputtering chamber was evacuated, to achieve a base pressure of 4×10^{-4} Pa. Oxygen was admitted to the deposition chamber through a flow controller. Oxygen flows of 6, 9, 12, 20, 26, and 32 sccm (standard cubic centimeter per minute) were used. These flow rates approximately correspond to 3.5, 5, 6.8, 11.3, 15, and 19×10^{-2} Pa gas pressures in non-sputtering conditions (the actual values were measured before each sputtering experiment). The film deposition was carried out using a mixture of O₂ and Ar gases at a total pressure of 2 Pa. The DC target potential that developed on the cathode during sputtering was kept constant via adjustment of the RF power. Three sets of samples were prepared using the DC target potentials of 1200 V, 1300 V, and 1400 V (corresponding to about 53 W, 65 W, and 70 W of RF power, respectively). The deposition time was 30 min for 1300 V and 1400 V, while it was 40 min for the 1200 V DC target potential. The target-to-substrate distance was about 50 mm, and the substrate holder was neither cooled nor heated during sputtering. For comparison purposes, a film was also deposited using a ceramic Ga₂O₃ target (Kurt J. Lesker, purity 99.99%). The sputtering of this reference sample was carried out at 1400 V (80 W) for 30 min, using 2 Pa Ar pressure. In all cases, the substrate was a piece of Si (100) single-crystal wafer.

2.2. Characterization

The structure of the films was investigated via X-ray diffraction (XRD), using a D8 Discover X-ray diffractometer (Bruker AXS, Karlsruhe, Germany) equipped with a Göbel mirror and a scintillation detector. The measurements were performed in parallel beam geometry between 15° and 90° of 2θ with Cu-Kα radiation. The X-ray beam dimension was 1 mm × 5 mm, while the 2θ step size and the scan speed were 0.02° and 2.5 s/step, respectively. The surface features of the samples were studied via scanning electron microscopy (SEM), using a Scios 2 dual-beam scanning electron microscope. Compositional variations were examined via backscattered electrons, and also via energy-dispersive spectroscopy (EDS). The EDS measurements were carried out on a 65 μm × 43 μm area, using an electron beam with 4.2 keV energy and 3.2 nA current. The error of composition, i.e., the error of the value x in Ga₂O_x, was ±0.38.

The composition of a sputtered layer was also determined via X-ray photoelectron spectroscopy (XPS), using Ecalab Xi+ equipment (Thermo Fisher Scientific, Waltham, MA, USA). The 1 cm-sized piece of sample was fixed with carbon sticking tape to the sample holder, and mounted to the UHV condition (1×10^{-8} Pa). As the “as received” state of the sample showed some organic contamination, which is usual for surfaces arriving from the free air condition, the sample was gradually cleaned in further steps, and checked between them. Avoiding damage to the layer beneath, possibly generated by the usual Ar⁺ beam sputtering, a mild Ar cluster beam was applied, to remove the adsorbed molecules such as carbohydrates, instead. The weak impact of the setup used (1000 atom clusters at 2 keV = >2 eV/atom) ensured that neither compositional nor chemical state changes took place via the cleaning procedure. The measured spot was chosen to be relatively large (900 μm), for good spectrum statistics. Spectra were detected at three different locations at an 0.6 eV energy resolution, with a 0.1 eV step size. The measured XPS spectra included the following peaks: Ga 2p 3/2 and 1/2 (1119 eV and 1146 eV), O 1s (532 eV), and C 1s (284 eV). The spectra were evaluated via determining the peak area. After the application of the usual Shirley background subtraction, the peak intensities were derived via Gaussian–Lorentzian fitting for the peak shapes. The component concentration was calculated with

sensitivity factors from the ALTHERMO1 library, assuming a homogeneous distribution of components.

The ellipsometric measurements were carried out on the specimens using a WOOL-LAM M2000U spectroscopic ellipsometer in the 190–1690 nm range, at an incidence of 70°. The evaluation of the data and the determination of the layer thickness and refractive index of the samples were performed using the CompleteEase software (version number is 5.15). The layers were modeled using the Tauc–Lorentz oscillator [24]. The thickness of the films using the above-described preparation conditions is in the range of 160 nm and 460 nm for the Ga target, and 160 nm for the ceramic target.

2.3. Model of Reactive Sputtering

The determination of the sputtering yields, i.e., the average number of sputtered atoms per incoming ion and the sticking coefficient, defined as the probability that an incoming neutral reactive gas molecule reacts with an unreacted metal atom at the surface, was carried out based on the Berg model. The original Berg model offers a relatively simple, analytical approach to describing the reactive sputtering process [22]. However, in some cases, the assumptions applied in the Berg model cannot adequately describe the reactive sputtering process; hence, an upgrade was introduced [23]. The upgraded Berg model includes additional mechanisms for the formation of the compound (besides chemisorption) on the target surface and subsurface; these are the direct implantation of reactive gas ions and the knock-in of already chemisorbed reactive gas atoms via the impact of Ar ions. The model assumes one surface layer on the target (which is not a monolayer) that incorporates all reactive gas atoms (either chemisorbed or implanted); this layer is also assumed to have a constant composition. The other important change compared to the original model consists of the assumption of the atomic sputtering of the compound, and the introduction of atomic sputtering yields. Next, a short summary of this upgraded model will be given.

Assuming a uniform partial pressure across the sputtering chamber, the flux of reactive gas molecules arriving to all the surfaces can be given according to the kinetic gas theory:

$$F = \frac{p}{\sqrt{2kT\pi m}}, \quad (1)$$

where p is the reactive gas partial pressure, k is the Boltzmann constant, T is the temperature in the chamber, and m is the mass of the reactive gas molecule, respectively.

In the steady state, the compound formation and removal are in equilibrium at the target, resulting in a constant surface coverage (θ_t). The balance equation for the target can be given as [23]:

$$\frac{J}{q} Y_k \theta_t^2 + \frac{J}{q} Y_c \theta_t = \frac{2}{z} \alpha_t F (1 - \theta_t) + \frac{2}{z} a_i \frac{J}{q} \left(\frac{p}{p_{tot}} \right) (1 - \theta_t), \quad (2)$$

where J is the ion current density, which is assumed to be uniformly distributed over the target surface; q is the elementary charge; and Y_k and Y_c are the knock-in yield and the partial sputtering yield of the reactive gas atoms in the compound, respectively. α_t is the sticking coefficient of the target; a_i is the probability that a reactive gas ion is implanted in the target; p_{tot} denotes the total pressure in the deposition chamber; and z represents the compound stoichiometry, i.e., $z = 3/2$ for Ga_2O_3 . It was assumed that oxygen and argon have the same ionization probability.

The surface coverage for the collecting area (θ_c), which is the net result of the material deposition from the target and the formation of the compound at the collecting surface, can also be defined. In the steady state, the corresponding balance equation can be given as:

$$\frac{2}{z} \alpha_c F (1 - \theta_c) A_c + \frac{1}{z} \frac{J}{q} Y_c \theta_t (1 - \theta_c) A_t = \frac{J}{q} [Y_{mc} \theta_t + Y_{mm} (1 - \theta_t)] \theta_c A_t, \quad (3)$$

where α_c is the sticking coefficient of the reactive gas on the collecting area; A_c and A_t are the surface area of the collecting surface and the target, respectively; and Y_{mc} and Y_{mm} are the partial sputtering yield of the metal in the compound and the sputtering yield of the unreacted metal, respectively.

Based on the above-described model, one can calculate the amount of deposited material. It is assumed that the deposited film only contains stoichiometric oxide, with a fraction of θ_c , and pure metal with a fraction of $(1 - \theta_c)$. θ_t and θ_c can be expressed using Equations (2) and (3). Thus, the thickness of the deposited layer can be given as follows:

$$d = \frac{J}{q} [Y_{mc}\theta_t + Y_{mm}(1 - \theta_t)] A_t \left((1 - \theta_c) \frac{M_m}{\rho_m} + \frac{\theta_c M_c}{2 \rho_c} \right) \frac{t}{NA_c} \quad (4)$$

where M_m (M_c) and ρ_m (ρ_c) are the molar mass and the density of the metal (compound), respectively; t is the duration of the deposition; and N is the Avogadro number. Note that the second term in the parenthesis is divided by 2, as a Ga_2O_3 molecule contains two gallium atoms.

Via deposition using different reactive gas flows, and by measuring the thickness of the forming layers, one can determine the sputtering yields of the target materials and the sticking coefficients. In our calculations, it is assumed that the sticking coefficients on the target and the collecting area are equal ($\alpha_t = \alpha_c = \alpha$), and that the reactive gas ions implanted in the subsurface have a sticking probability of unity ($\alpha_i = 1$). The current density was calculated based on the DC target potential, the sputtering power, and the surface area of the target ($A_t = 44 \text{ cm}^2$). The temperature in the deposition chamber was estimated to be 330 K, based on an earlier study [25]. The collecting area ($A_c = 115 \text{ cm}^2$) was determined via measuring the area of the deposition pattern inside the sputtering chamber. The material was assumed to be uniformly deposited on the collecting area.

3. Results and Discussion

Figure 2 presents a typical example of the XRD pattern of the sputtered films. No crystalline peaks can be found, except the reflections of the Si substrate. Similar results were obtained for other samples, as well, regardless of the deposition conditions. Thus, the films in this work can be identified as X-ray-amorphous, as is often the case for RF sputtered films deposited at room temperature [5,11,15].

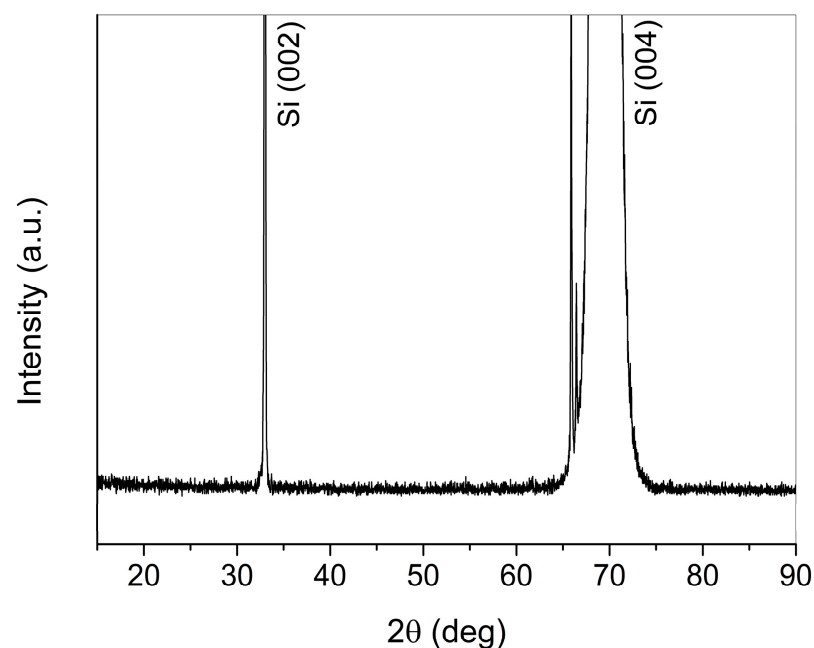


Figure 2. A typical XRD pattern of the RF sputtered films; only the crystalline peaks of the substrate can be identified.

The oxygen content of the sputtered films, measured via EDS, is shown in Figure 3 as a function of the oxygen partial pressure (detailed EDS results can also be found in Tables S1–S3 of the Supplementary Materials). The measurements confirm that a gallium oxide layer can be grown via reactive sputtering, using a liquid gallium target. The oxygen content of the films is slightly below the nominal Ga_2O_3 stoichiometry value, even for the highest applied oxygen flow. Nevertheless, the sample sputtered using 1200 V and 32 sccm of oxygen (0.19 Pa of O_2 pressure) presents a higher O/Ga atomic ratio than a non-reactively sputtered gallium oxide film grown using a ceramic Ga_2O_3 target. As shown in Figure 3, increasing the oxygen partial pressure results in only slight changes in the oxygen content. A small effect of the DC target potential in the composition of the Ga_2O_x films can be seen only for the lowest oxygen pressures; i.e., an increase in the DC target potential decreases the oxygen content of the layers.

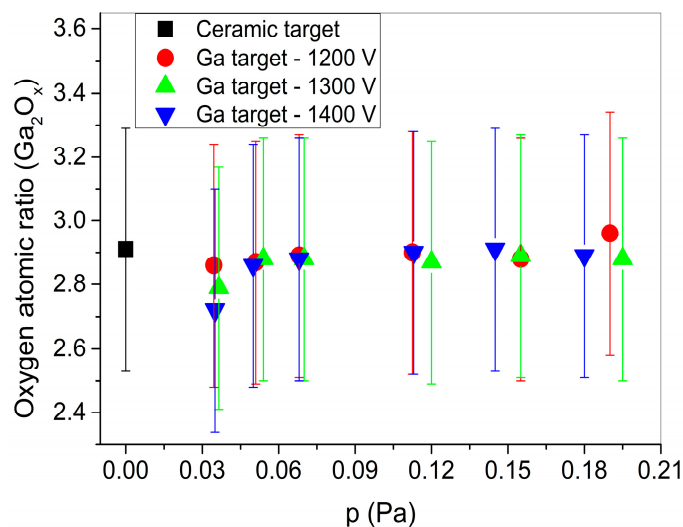


Figure 3. The oxygen atomic ratio of the sputtered gallium oxide films, determined via EDS, as a function of the oxygen partial pressure.

For reference, the composition of the sample prepared at 1300 V and 32 sccm (0.19 Pa of O_2 pressure) was also measured via XPS. Figure 4 shows the recorded spectrum, including the main peaks of Ga and O. No elements other than gallium and oxygen were observed on the cleaned surface. The calculated concentration of Ga at the three measured positions was identical within 1%, which resulted in $X = 2.76$ after its conversion to Ga_2O_x form. It confirms the EDS data within the expected error.

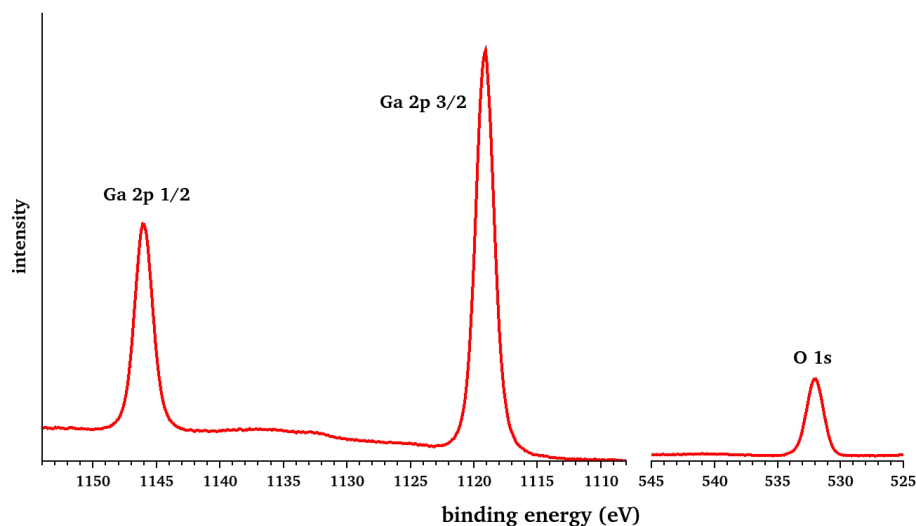


Figure 4. The XPS peaks of the Ga-oxide layer deposited at 1300 V and 32 sccm (0.19 Pa O_2).

Sputtering using 1400 V DC target potential resulted in the formation of a few metallic-looking droplets on the surface of the samples that were even observable via an optical microscope. A backscattered electron micrograph of such a droplet is shown on Figure 5. It is evident from the image that the droplet has a higher average atomic number than the surrounding area. This was confirmed via EDS, which proved that the droplet mainly contains gallium, and only a minimal amount of oxygen. Note, however, that these droplets were found only occasionally and, apart from them, the samples show a homogeneous composition on the scale investigated via SEM-EDS (see the backscattered electron image of Figure S1 of the Supplementary Materials). Furthermore, such surface features could not be observed for the films prepared at 1200 V or 1300 V. Thus, using a lower DC target potential, i.e., a lower sputtering power, offers the benefit of better film quality.

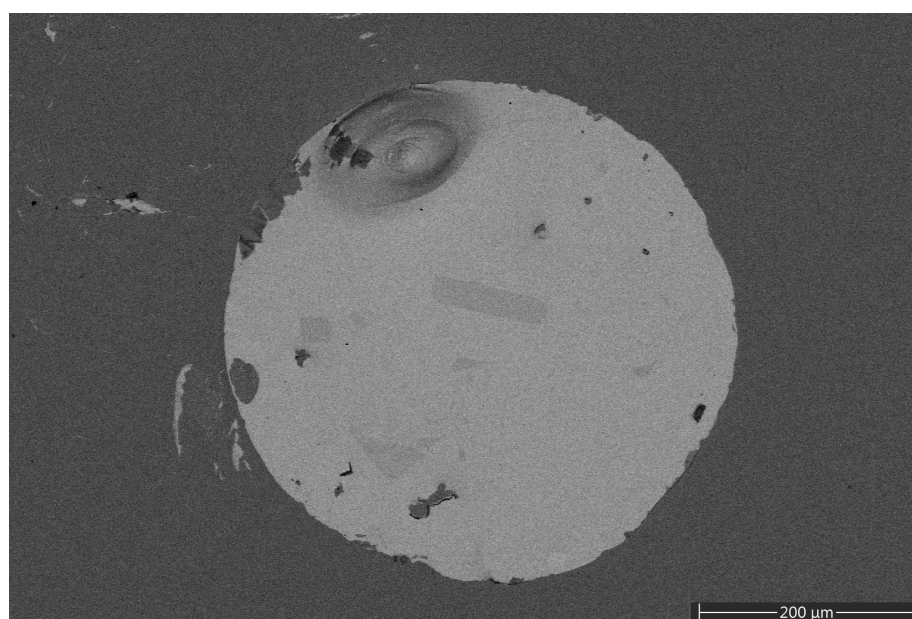


Figure 5. The backscattered electron micrograph of a gallium droplet on the sample prepared using 6 sccm (0.035 Pa) oxygen at 1400 V.

Figure 6a shows the refractive indices (n) and extinction coefficients (k) of the reactively sputtered (at 1400 V DC target potential) gallium oxide layers as a function of the wavelength, determined via spectroscopic ellipsometry (for additional information, see Figure S2 and Table S4 of the Supplementary Materials). In general, the films prepared using an oxygen flow of 9–32 sccm have similar n and k values. It is noteworthy that the extinction coefficient becomes zero in the UV range at 300 nm; thus, it has potential for solar-blind applications. The sample deposited at an oxygen flow of 6 sccm (0.035 Pa partial pressure) shows a higher refractive index in most of the studied wavelength range, and its k value also cuts off at a higher wavelength (400 nm). Similar observations were also made for the films sputtered at a 1300 V DC target potential; however, at 1200 V, only slight differences could be observed between the optical parameters of the different samples (see Figure S3 of the Supplementary Materials). This behavior can be interpreted in terms of the oxygen content of these layers, if the refractive index (at 632.8 nm) is plotted as a function of the oxygen atomic ratio (see Figure 6b). A general trend in the value of n can be observed, namely that the layers with a higher oxygen content, i.e., closer to the Ga_2O_3 stoichiometry, present lower refractive indices. The measured values are comparable to the refractive indices of gallium oxide thin films prepared via other deposition techniques, such as plasma-enhanced atomic layer deposition ($n = 1.78$ – 1.88 , depending on the oxygen partial pressure) [26] and electron-beam evaporation ($n = 1.85$) [27].

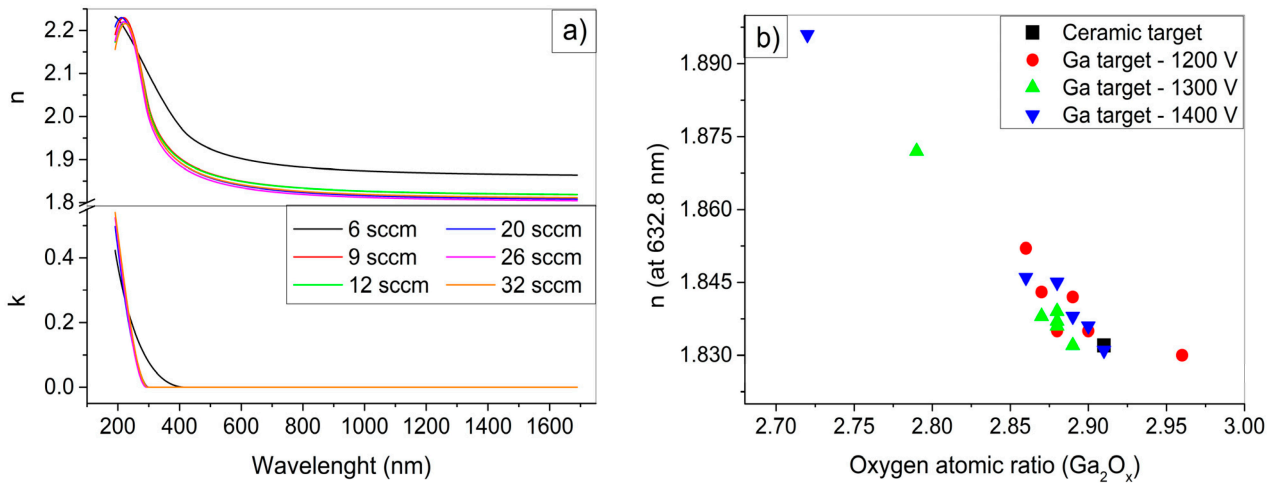


Figure 6. The refractive indices (n) and extinction coefficients (k) as a function of the wavelength for the samples sputtered at a 1400 V DC target potential (a). The refractive indices (at 632.8 nm) of the gallium oxide films as a function of the oxygen atomic ratio (b).

Figure 7 shows the thickness of the deposited films, determined via spectroscopic ellipsometry, at different oxygen partial pressures. Note that, for the 1200 V samples, a 40 min deposition time was used, instead of 30 min. If one compares these thickness data to the thickness of the reference sample sputtered from the ceramic target ($d_{\text{ref}} = 160 \text{ nm}$), it is evident that significantly higher deposition rates can be achieved using a liquid Ga target, while maintaining a similar composition. To be specific, using the liquid Ga target and 20 sccm O_2 flow (0.113 Pa O_2 pressure), 9.4 nm/min (for 1400 V), and 5.5 nm/min (for 1200 V) deposition rates were achieved; while using the ceramic target (1400 V), only a 5.3 nm/min deposition rate was measured.

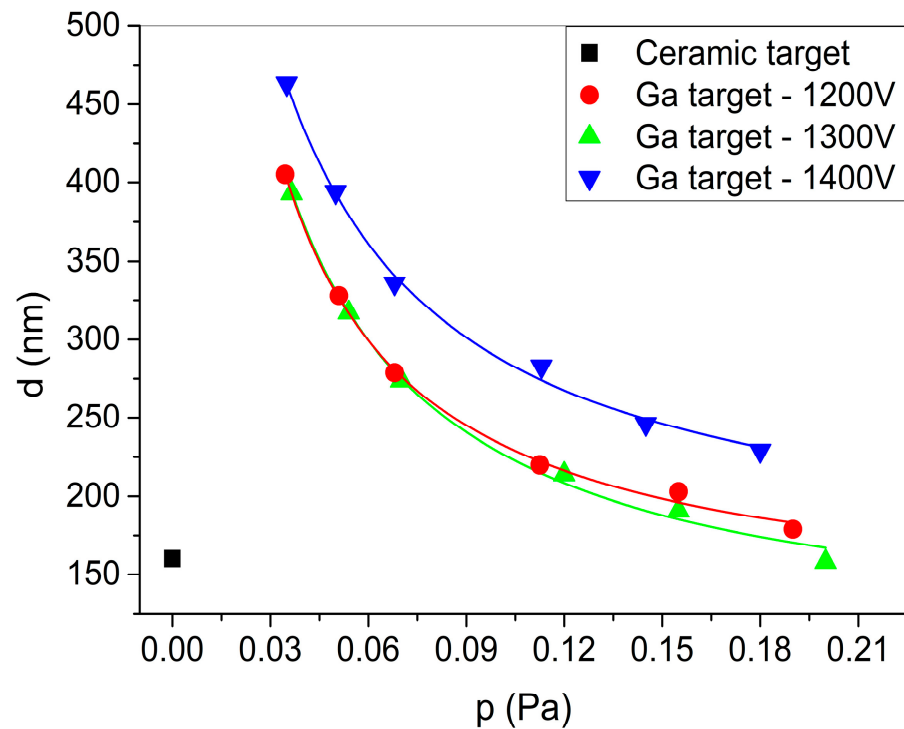


Figure 7. The film thickness at different oxygen partial pressures and DC target potentials, as measured via ellipsometry, and the fit to the data points (solid lines), using Equation (4).

Visual inspection of the target after sputtering shows islands of oxide on its surface (see the whitish areas on top of the target, Figure 1a,b). An increased oxygen admission results in a higher coverage, as can be seen through comparing Figures 1a and 1b. Such a pattern was also observed in an earlier report that demonstrated that oxide forms islands with fractal-like structures on the liquid Ga surface [28]. It is most probable that such a visually observable oxide layer is more than one monolayer thick. Thus, the assumption of the original Berg model that only a monolayer of the compound exists on the surface does not hold. Hence, the calculations to derive the sputtering yields and sticking coefficient were based on the upgraded Berg model. The solid lines in Figure 7 show the fit of the thickness data using Equation (4), according to the model presented in Section 2.3. Here, the reactive gas partial pressure data measured before the sputtering experiment were used, instead of the actual reactive gas pressure, as this could not be measured in our experimental setup during sputtering. The fitted parameters are given in Table 1. The sputtering yield of Ga (Y_{mm}) is close to the values estimated using SRIM simulations [29], i.e., 1.9, 2.04 and 2.15 for 1200 V, 1300 V, and 1400 V, respectively. As expected, the partial sputtering yields are significantly lower than the sputtering yield of pure gallium. Increasing the DC target potential (and, consequently, increasing the sputtering power) results in increased Ga yields; however, the partial sputtering yield of oxygen atoms decreased while their knock-in yield increased. This means that, at higher DC target potentials, due to the more energetic incoming ions, the knock-in implantation mechanism becomes more and more significant, compared to the case of 1200 V. This also leads to an increase of the preferential sputtering in favor of Ga with the increase of the DC target potential. The sticking coefficient shows a decreasing tendency upon the increase in the DC target potential. The value of the sticking coefficient can also be estimated based on the electronegativity difference of the constituting elements, as presented in ref. [30] for different metal and oxygen systems. Accordingly, the expected value is around 0.03 for the Ga-O system [30], which is comparable to the result of the fitting based on the upgraded Berg model.

Table 1. Fitted sputtering parameters.

Parameter	1200 V	1300 V	1400 V
Y_{mm}	1.9 ± 0.3	2.0 ± 0.3	2.0 ± 0.2
Y_{mc}	0.081 ± 0.006	0.07 ± 0.01	0.11 ± 0.01
Y_c	0.06 ± 0.03	0.03 ± 0.02	0.01 ± 0.01
Y_k	0.03 ± 0.02	0.05 ± 0.03	0.07 ± 0.02
α	0.036 ± 0.009	0.025 ± 0.005	0.024 ± 0.004

Based on the above findings, the main benefit of the liquid Ga target compared to the ceramic Ga₂O₃ target lies in the higher deposition rate. The ability to control the composition, i.e., the oxygen content, of the deposited film by changing the oxygen flow rate (see Figure 3) can also be considered an advantage. On the other hand, liquid Ga is more difficult to manipulate, and can only be used in a configuration where the target can be placed at the bottom of the sputtering chamber.

4. Conclusions

A liquid Ga target was used to sputter deposit gallium oxide thin films in a radio frequency sputtering device. Different oxygen flows and DC target potentials were tested, to explore the dependence of the composition on the deposition conditions. It was shown that the application of lower DC target potentials may be beneficial, to prepare films with a higher oxygen content and better film quality. Using a high enough oxygen inflow, it is possible to achieve a composition closer to stoichiometry than in the case of a non-reactively sputtered ceramic Ga₂O₃ target. It was also demonstrated that higher deposition rates can be achieved via the reactive sputtering of a liquid target, compared to the use of a ceramic one. The modeling of the reactive sputtering process was carried out based on the Berg model. The partial sputtering yields, the knock-in yield, and the sticking coefficient were

determined. According to the fitted yield parameters, preferential sputtering becomes more significant as the DC target potential increases.

Supplementary Materials: The following supporting information can be downloaded at: <https://www.mdpi.com/article/10.3390/coatings13091550/s1>, Figure S1. Secondary electron image (a), backscattered electron image (b) and the corresponding EDS spectrum (c) of the sample prepared at 1400 V DC target potential and 26 sccm oxygen flow (0.14 Pa partial pressure); Figure S2. The measured ellipsometry data (Psi and Delta parameters) as a function of wavelength and the fitted model curves for the sample prepared at 1400 V and 32 sccm; Figure S3. Refractive indices (n) and extinction coefficients (k) as a function of wavelength for the gallium oxide films prepared at different conditions; Table S1. Atomic percent of the constituting elements of the samples prepared at 1200 V DC target potential determined by EDS; Table S2. Atomic percent of the constituting elements of the samples prepared at 1300 V DC target potential determined by EDS; Table S3. Atomic percent of the constituting elements of the samples prepared at 1400 V DC target potential determined by EDS; Table S4. MSE (mean squared error) values of the fitted ellipsometry curves.

Author Contributions: Conceptualization, M.G. and M.S.; methodology, M.G. and M.S.; investigation, M.G., T.K., A.S. and Z.E.H.; writing—original draft preparation, M.G.; writing—review and editing, M.S. and B.P.; visualization, M.G. All authors have read and agreed to the published version of the manuscript.

Funding: This research was carried out in the framework of the project New Semiconductor Materials, TKP2021-NKTA-05, and was also funded by the Hungarian Scientific Research Fund OTKA, Grant number: K143216.

Institutional Review Board Statement: Not applicable.

Informed Consent Statement: Not applicable.

Data Availability Statement: The data presented in this study are available in the Supplementary Materials.

Acknowledgments: The authors thank György Sáfrán for his help in fabricating the Ni target holder.

Conflicts of Interest: The authors declare no conflict of interest. The funders had no role in the design of the study; in the collection, analyses, or interpretation of data; in the writing of the manuscript; or in the decision to publish the results.

References

1. Pearton, S.J.; Yang, J.; Cary, P.H., IV; Ren, F.; Kim, J.; Tadjer, M.J.; Mastro, M.A. A Review of Ga₂O₃ Materials, Processing, and Devices. *Appl. Phys. Rev.* **2018**, *5*, 011301. [CrossRef]
2. Galazka, Z. β -Ga₂O₃ for Wide-Bandgap Electronics and Optoelectronics. *Semicond. Sci. Technol.* **2018**, *33*, 113001. [CrossRef]
3. Wang, J.; Ye, L.; Wang, X.; Zhang, H.; Li, L.; Kong, C.; Li, W. High Transmittance β -Ga₂O₃ Thin Films Deposited by Magnetron Sputtering and Post-Annealing for Solar-Blind Ultraviolet Photodetector. *J. Alloys Compd.* **2019**, *803*, 9–15. [CrossRef]
4. Lin, H.-J.; Gao, H.; Gao, P.-X. UV-Enhanced CO Sensing Using Ga₂O₃-Based Nanorod Arrays at Elevated Temperature. *Appl. Phys. Lett.* **2017**, *110*, 043101. [CrossRef]
5. Saikumar, A.K.; Nehate, S.D.; Sundaram, K.B. Review—RF Sputtered Films of Ga₂O₃. *ECS J. Solid State Sci. Technol.* **2019**, *8*, Q3064. [CrossRef]
6. Sasaki, K.; Kuramata, A.; Masui, T.; Villora, E.G.; Shimamura, K.; Yamakoshi, S. Device-Quality β -Ga₂O₃ Epitaxial Films Fabricated by Ozone Molecular Beam Epitaxy. *Appl. Phys. Express* **2012**, *5*, 035502. [CrossRef]
7. Mezzadri, F.; Calestani, G.; Boschi, F.; Delmonte, D.; Bosi, M.; Fornari, R. Crystal Structure and Ferroelectric Properties of ϵ -Ga₂O₃ Films Grown on (0001)-Sapphire. *Inorg. Chem.* **2016**, *55*, 12079–12084. [CrossRef]
8. Murakami, H.; Nomura, K.; Goto, K.; Sasaki, K.; Kawara, K.; Thieu, Q.T.; Togashi, R.; Kumagai, Y.; Higashiwaki, M.; Kuramata, A.; et al. Homoepitaxial Growth of β -Ga₂O₃ Layers by Halide Vapor Phase Epitaxy. *Appl. Phys. Express* **2014**, *8*, 015503. [CrossRef]
9. Zhao, M.; Tong, R.; Chen, X.; Ma, T.; Dai, J.; Lian, J.; Ye, J. Ellipsometric Determination of Anisotropic Optical Constants of Single Phase Ga₂O₃ Thin Films in Its Orthorhombic and Monoclinic Phases. *Opt. Mater.* **2020**, *102*, 109807. [CrossRef]
10. Meng, Y.; Gao, Y.; Chen, K.; Lu, J.; Xian, F.; Xu, L.; Zheng, G.; Kuang, W.; Cao, Z. Annealing Induced Phase Transition and Optical Properties of Ga₂O₃ Thin Films Synthesized by Sputtering Technique. *Optik* **2021**, *244*, 167515. [CrossRef]
11. Mobbakeri, S.; Akaltun, Y.; Özer, A.; Kılıç, M.; Tüzemen, E.Ş.; Gür, E. Gallium Oxide Films Deposition by RF Magnetron Sputtering; a Detailed Analysis on the Effects of Deposition Pressure and Sputtering Power and Annealing. *Ceram. Int.* **2021**, *47*, 1721–1727. [CrossRef]

12. Li, S.; Jiao, S.; Wang, D.; Gao, S.; Wang, J. The Influence of Sputtering Power on the Structural, Morphological and Optical Properties of β -Ga₂O₃ Thin Films. *J. Alloys Compd.* **2018**, *753*, 186–191. [[CrossRef](#)]
13. Li, M.-Q.; Yang, N.; Wang, G.-G.; Zhang, H.-Y.; Han, J.-C. Highly Preferred Orientation of Ga₂O₃ Films Sputtered on SiC Substrates for Deep UV Photodetector Application. *Appl. Surf. Sci.* **2019**, *471*, 694–702. [[CrossRef](#)]
14. Jiao, S.; Lu, H.; Wang, X.; Nie, Y.; Wang, D.; Gao, S.; Wang, J. The Structural and Photoelectrical Properties of Gallium Oxide Thin Film Grown by Radio Frequency Magnetron Sputtering. *ECS J. Solid State Sci. Technol.* **2019**, *8*, Q3086. [[CrossRef](#)]
15. Akazawa, H. Formation of Various Phases of Gallium Oxide Films Depending on Substrate Planes and Deposition Gases. *Vacuum* **2016**, *123*, 8–16. [[CrossRef](#)]
16. Cha, S.Y.; Kim, D.; Lim, H.; Mun, B.S.; Noh, D.Y.; Kang, H.C. Characterization of Non-Stoichiometric Ga₂O_{3-x} Thin Films Grown by Radio-Frequency Powder Sputtering. *Ceram. Int.* **2021**, *47*, 3238–3243. [[CrossRef](#)]
17. Patil, V.; Lee, B.-T.; Jeong, S.-H. Optical and Structural Characterization of High Crystalline β -Ga₂O₃ Films Prepared Using an RF Magnetron Sputtering. *J. Alloys Compd.* **2022**, *894*, 162551. [[CrossRef](#)]
18. Liao, Y.; Jiao, S.; Li, S.; Wang, J.; Wang, D.; Gao, S.; Yu, Q.; Li, H. Effect of Deposition Pressure on the Structural and Optical Properties of Ga₂O₃ Films Obtained by Thermal Post-Crystallization. *CrystEngComm* **2017**, *20*, 133–139. [[CrossRef](#)]
19. Singh, A.K.; Gupta, M.; Sathe, V.; Katharria, Y.S. Effect of Annealing Temperature on β -Ga₂O₃ Thin Films Deposited by RF Sputtering Method. *Superlattices Microstruct.* **2021**, *156*, 106976. [[CrossRef](#)]
20. Dong, L.; Jia, R.; Xin, B.; Zhang, Y. Effects of Post-Annealing Temperature and Oxygen Concentration during Sputtering on the Structural and Optical Properties of β -Ga₂O₃ Films. *J. Vac. Sci. Technol. A* **2016**, *34*, 060602. [[CrossRef](#)]
21. Zubkins, M.; Vibornijs, V.; Strods, E.; Butanovs, E.; Bikse, L.; Ottosson, M.; Hallén, A.; Gabrusenoks, J.; Purans, J.; Azens, A. Deposition of Ga₂O₃ Thin Films by Liquid Metal Target Sputtering. *Vacuum* **2023**, *209*, 111789. [[CrossRef](#)]
22. Berg, S.; Nyberg, T. Fundamental Understanding and Modeling of Reactive Sputtering Processes. *Thin Solid Film.* **2005**, *476*, 215–230. [[CrossRef](#)]
23. Berg, S.; Särhammar, E.; Nyberg, T. Upgrading the “Berg-Model” for Reactive Sputtering Processes. *Thin Solid Film.* **2014**, *565*, 186–192. [[CrossRef](#)]
24. Jellison, G.E.; Modine, F.A. Parametrization of the optical functions of amorphous materials in the interband region. *Appl. Phys. Lett.* **1996**, *69*, 371. [[CrossRef](#)]
25. Hegedüs, N.; Balázs, C.; Kolonits, T.; Olasz, D.; Sáfrán, G.; Serényi, M.; Balázs, K. Investigation of the RF Sputtering Process and the Properties of Deposited Silicon Oxynitride Layers under Varying Reactive Gas Conditions. *Materials* **2022**, *15*, 6313. [[CrossRef](#)] [[PubMed](#)]
26. Liu, W.; He, J.; Zhu, X.; Huang, T.; Chen, X.; Zheng, Y.; Chen, L.; Zhang, R. Thickness Dependent Optical Properties of Amorphous/Polycrystalline Ga₂O₃ Thin Films Grown by Plasma-Enhanced Atomic Layer Deposition. *Thin Solid Film.* **2023**, *766*, 139655. [[CrossRef](#)]
27. Li, S.; Yang, C.; Zhang, J.; Dong, L.; Cai, C.; Liang, H.; Liu, W. Tunable Optical Properties of Amorphous-Like Ga₂O₃ Thin Films Deposited by Electron-Beam Evaporation with Varying Oxygen Partial Pressures. *Nanomaterials* **2020**, *10*, 1760. [[CrossRef](#)]
28. Chabala, J.M. Oxide-Growth Kinetics and Fractal-like Patterning across Liquid Gallium Surfaces. *Phys. Rev. B* **1992**, *46*, 11346–11357. [[CrossRef](#)]
29. Ziegler, J.F.; Ziegler, M.D.; Biersack, J.P. SRIM—The Stopping and Range of Ions in Matter. In *Nuclear Instruments and Methods in Physics Research Section B: Beam Interactions with Materials and Atoms*; Elsevier: Amsterdam, The Netherlands, 2012.
30. Leroy, W.P.; Mahieu, S.; Persoons, R.; Depla, D. Quantification of the Incorporation Coefficient of a Reactive Gas on a Metallic Film during Magnetron Sputtering: The Method and Results. *Thin Solid Film.* **2009**, *518*, 1527–1531. [[CrossRef](#)]

Disclaimer/Publisher’s Note: The statements, opinions and data contained in all publications are solely those of the individual author(s) and contributor(s) and not of MDPI and/or the editor(s). MDPI and/or the editor(s) disclaim responsibility for any injury to people or property resulting from any ideas, methods, instructions or products referred to in the content.